DYNAMIC MODELING OF SERIES VECTORIAL COMPENSATOR

By

K. HIMAJA * T. S. SURENDRA ** S. TARA KALYANI ***

* Lecturer, Department of Technical Education, Government of Andhra Pradesh, India.
** Director, Visionary Lighting and Energy India (P) Ltd, Hyderabad, India.
*** Controller of Examinations and Professor, Department of Electrical and Electronics Engineering, JNTU Hyderabad, India.

Date Received: 26/05/2018 Date Revised: 17/08/2018 Date Accepted: 28/08/2018

ABSTRACT

This study presents the theory and modelling of a novel controller based on PWM - based Series Vectorial Compensator (SVeC). This is a new series Flexible AC Transmission System (FACTS) controller for active power flow control in a transmission line and damping of low-frequency oscillations (LFO). This paper presents the basic module, steady- state operation, mathematical analysis, current injection model, and dynamic model of SVeC. The main contribution of this study is that a current injection model of the SVeC for studying the effect of the SVeC on the LFO is proposed. A brief comparison of the Coordinated Control (COC) of SVeC and Power System Stabilizer (PSS) without control is presented for dynamic series compensation of transmission lines. The multi machine network is used for comparison purpose. The performance of the proposed controller is checked through eigen-value analysis and non-linear time domain simulations under nominal load operation. The obtained results show that the proposed control is efficient for studying the effects of SVeC on the electro mechanical oscillations and it has better oscillation damping characteristics than without control.

Keywords: SVeC and PSS, Coordinated - Control, Low Frequency Oscillations.

INTRODUCTION

The Series Vectorial Compensator (SVeC) was proposed for the Flexible AC Transmission Systems (FACTS), with primary duty like power flow and the secondary functions to be oscillation damping, voltage control, etc (Lopes & Joos, 2001; Venkataramanan & Johnson, 2002; Gonzalez et al., 2010; Mancilla-David et al., 2008). As, SVeC has till now practically not been designed in the market and placed in a EPS. The operation of SVeC with PID to supress LFO in a simple system was explained in (Truong & Wang, 2013). Application of SVeC with SSSC to damp LFO was presented in (Wang & Truong, 2012). Safari et al. (2016) have presented the COC of PWMSC and PSS for damping LFO in multimachine networks using dynamic index. A brief comparison of SVeC with TCSC to a simple system was presented by (Himaja et al. 2016), where it shows that SVeC is smoother control alternative than the TCSC. Dynamic stability analysis of SVeC with different damping controllers is demonstrated for different case studies (Sadikovic, 2004). Pal and Chaudhuri (2006) have discussed the systematic comparison of cost and switching function of SVeC with SSSC.

1. SVeC

1.1 Basic Module of SVeC

Fixed series capacitor is the most economical solution for increasing power transfer in long transmission lines. Latest developments in power electronics introduce the use of FACTS technology in Electrical Power Systems (EPS) for fast power flow control. SVeC can be designed to modify the line reactance and damp the LFO in a network. Figure 1 displays a schematic diagram of the SVeC which is connected into a transmission line.

The schematic of SVeC connected in the transmission line is shown in Figure 1. SVeC has primary switches S_{1a}, S_{2a}, S_{1b}, S_{2b} , S_{1c} , and S_{2c}, and C_a, C_b, and C_z are the series compensated capacitors.

The operation of SVeC is presented in (Wang & Truong, 2012; Himaja et al. 2016). In Figure 1, primary side of capacitors are connected in Y and the secondary side of

www.manaraa.com

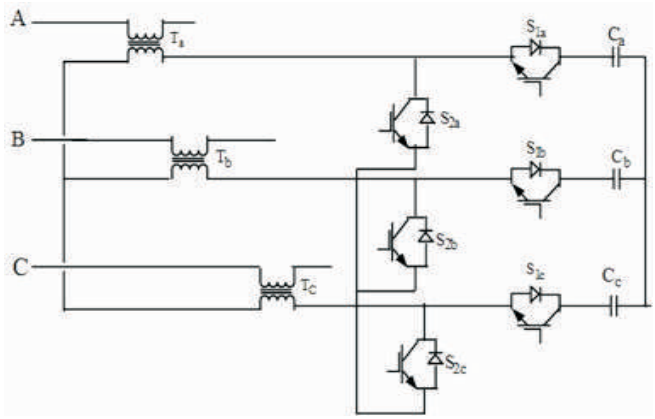

Figure 1. SVeC Inserted in a Transmission Line

coupling transformer is connected in Δ.

The compensator controls the degree of series reactance by varying the duty ratio of SVeC. The purpose of series compensator is to control the real power in a network with a simple structure that provides a means for controlling continuously the degree of reactance through the variation of duty ratio (Lopes & Joos, 2001).

1.2 Operation of SVeC

The SVeC is assumed to be connected between buses 1 and 2 as shown in Figure 2, where SVeC is operated like a series controllable reactance. To model a control strategy of SVeC, it is useful to have a proper design representation for SVeC.

Figure 2 is the single line diagram SVeC of Figure 1. The proposed SVeC is located between bus 1 and 2 as displayed in Figure 2. A transmission line having a reactance X_{12} and the reactance of SVeC is XSVeC is represented in Figure 2. In transformer's secondary side, series compensated capacitors and SVeC converter are placed. From Figure 2, the equal reactance of bus 1 and 2 (Gonzalez et al., 2010) is as follows.

$$X_{eq} = X_{12} + X_{SVeC} \quad (1)$$

where

$$X_{SVeC} = -n^2(1 - D_s)^2 X_C \quad (2)$$

where n is the turns ratio of transformer, duty ratio of SVeC converter is D_s and it is ratio of on period to the total time period.

1.3 Mathematical Analysis of SVeC

For analyzing the SVeC, the single phase equivalent

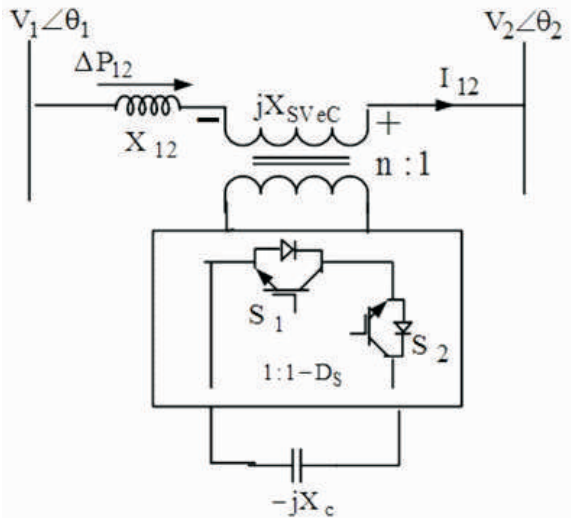

Figure 2. Single Line Diagram of SVeC

model as shown in Figure 3 is used. The primary series transformer is represented by a leakage reactance (X_P) in series with an ideal transfomer at the transmission line. In the secondary side, there is a SVeC converter and a bank of capacitors with reactance X_C. The equivalent and injected reactances at the transmission line may be calculated as follows (Venkataramanan & Johnson, 2002).

$$X_{eq} = X_{12} + X_P + X_{SVeC} \quad (3)$$

1.4 SVeC Current Injection Model

The current injection model, which can be used for small signal stability and transient stability studies, is obtained by replacing the voltage across the SVeC with the current source. This model is helpful for understanding the effect and performance of the SVeC on system damping enhancement (Sadikovic, 2004).

A SVeC connected between nodes 1 and 2 in a transmission line is shown in Figure 3, where SVeC is simplified like a continuously capacitive controllable reactance and its equivalent circuit is represented in Figure 4. In Figures 3 and 4, $V_1\angle\theta_1$ and $V_2\angle\theta_2$ are the complex voltages at nodes 1 and 2, and $V_{SVeC} = -j\,X_{SVeC}I_{12}$ represents a voltage across the SVeC.

From Figure 3,

$$I_{12} = \frac{V_1 - V_2}{R_{12} + j(X_{12} + X_{eq})} \quad (4)$$

$$I_{12} = \frac{V_1 - V_2}{R_{12} + j(X_{12} + X_P - K^2(1 - D_S)^2 X_C)} \quad (5)$$

www.manaraa.com

The current injection model of the SVeC is obtained by replacing the volatge across the SVeC by an equivalent current source, I_{se}, in Figure 5. Then,

$$I_{12} = \frac{V_{SVeC}}{R_{12}+jX_{12}} = -\frac{jX_{SVeC}I_{12}}{R_{12}+jX_{12}} \quad (6)$$

1.5 Dynamic Current Model of SVeC

Figure 6 shows a schematic diagram of the dynamic model of SVeC for typical oscillatory stability studies. It can be noticed that following a similar modeling approach as in the case of the other series compensator, the line reactance is assumed to be controlled through the duty cycle D_s.

Firstly, this modeling, power oscillation damping controller is not considered. The model includes an input signal and a reference model $X_{SVeC\ ref}$, which is the initial value of the series compensator. These inputs are summed to produce an error signal, which is fed into a first-order lag block. The lag block is associated with the duty cycle control and natural response of the SVeC and is represented by a single time constant T_{SVeC}. The output of the lag block X_{SVeC} has windup limits associated with it. The ultimate reactance value is used to modify the line impedance of the series branch compensated during the calculation of the network solution (Pal & Chaudhuri, 2006; Padiyar, 1996). Besides a dynamic controller, the SVeC has to be equipped with a POD stabilizer adequately designed.

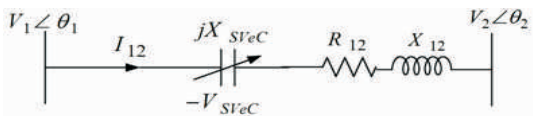

Figure 3. SVeC placed in a Transmission Line

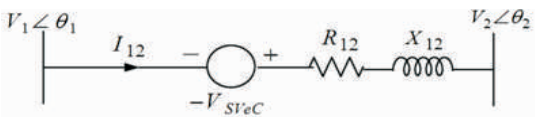

Figure 4. SVeC Equivalent Circuit

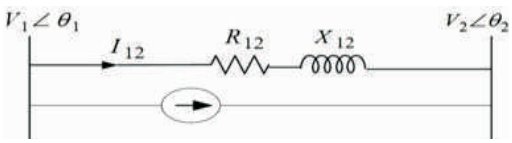

Figure 5. Replace the Voltage Source V_{SVeC} by a Current Source

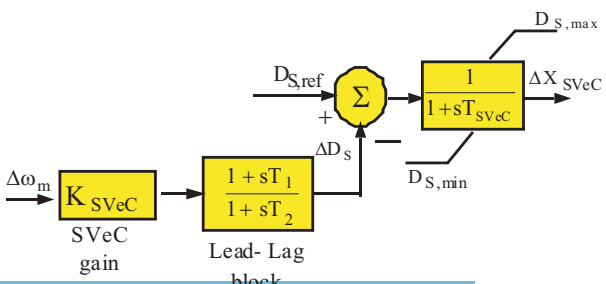

Figure 6. Block Diagram of SVeC Damping Controller

2. COC of SVeC and PSS

2.1 PSS

The general block diagram of PSS damping controller is shown in Figure 7. It has gain and lead-lag compensator blocks (Kundur et al., 1994). Gain block provides adequate damping to the input signal. The block diagram transfer function of PSS is,

$$\frac{V_S}{\Delta\omega_m} = K_{PSS}\left(\frac{1+sT_1}{1+sT_2}\right) \quad (7)$$

where T_1 and T_2 are lead-lag time constants, which are similar to SVeC damping controller. To damp the LFO ΔV_s is combined with Δv_{ref}.

ΔV_{Si} is the state equation corresponding to PSS as,

$$\Delta\dot{V}_{Si} = -\frac{1}{T_2}\Delta V_{Si} + \frac{K_{PSS}}{T_2}\frac{\Delta\omega_i}{\omega_S} + \frac{K_{PSS}T_1}{T_2}\frac{\Delta\dot{\omega}_i}{\omega_S} \quad (8)$$

$$\Delta X_i = \left[\Delta\delta_i\ \Delta\omega_i\ \Delta E'_{qi}\ \Delta E'_{di}\ \Delta E_{fdi}\ \Delta V_{Ri}\ \Delta R_{Fi}\ \Delta V_{Si}\right] \quad (9)$$

In ΔX_i, the state variable ΔV_{Si} corresponds to PSS.

Therefore, the system matrix A_PSS for a study network is [A_PSS](7m+1)×(7m+1). So, test system's eigenvalues will be increased by one (Kundur et al., 1994).

2.2 COC of SVeC and PSS

When SVeC is inserted in the network, the state variables corresponding to the SVeC damping controller $[\Delta D_S\ \Delta X_{SVeC}]^T$ are included with the generator state equations is,

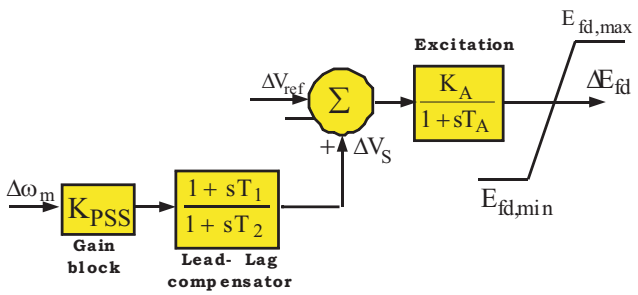

Figure 7. Block Diagram of PSS

www.manaraa.com

$$\Delta \dot{D}_S = \frac{K_{SVeC} T_1}{T_2} \frac{K_2}{2H} \Delta E'_q + \frac{K_{SVeC} T_1}{T_2} \frac{K_1}{2H} \Delta\delta + \left(-\frac{K_{SVeC}}{T_2} + \frac{K_{SVeC} T_1}{T_2} \frac{D\omega_S}{2H}\right) \Delta\omega + \left(-\frac{1}{T_2} + \left(\frac{-K_{SVeC} T_1 K_{DS}}{2HT_2}\right)\right) \Delta D_S - \frac{K_{SVeC} T_1}{2HT_2} \Delta T_M \quad (10)$$

$$\Delta \dot{X}_{SVeC} = -\frac{1}{T_{SVeC}} \Delta D_S - \frac{1}{T_{SVeC}} \Delta X_{SVeC} \quad (11)$$

whereas,

$$K_2 = \frac{\partial P_e}{\partial E'_q}, K_1 = \frac{\partial P_e}{\partial \delta} \text{ and } K_{D_S} = \frac{\partial P_e}{\partial D_S}$$

where P_e is the electrical power.

The installation of SVeC results as,

$$\Delta X_i = \left[\Delta\delta_i \; \Delta\omega_i \; \Delta E'_{qi} \; \Delta E'_{di} \; \Delta E_{fdi} \; \Delta V_{Ri} \; \Delta R_{Fi} \; \Delta D_{Si} \; \Delta X_{SVeCi}\right]$$

for the i_{th} generator for which SVeC control unit receives input signal ($\Delta\omega$). In ΔX_i, ΔD_{si} and ΔX_{SVeCi} are the state variables of the SVeC damping controller.

In order to improve the dynamic stability of the network, the block diagram for COC of SVeC and PSS is given in Figure 8. In COC of SVeC and PSS, the state variables ΔV_{si}, ΔD_{si}, ΔX_{SVeCi} are the PSS, SVeC controllers. The total eigenvalues will be 26.

3. Simulation Results and Discussions

The system W.S.C.C 3 machine, 9 bus is used for test system. Figure 9 shows the COC of SVeC and PSS

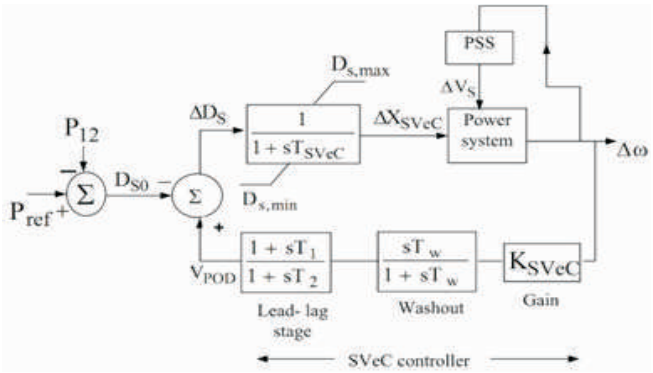

Figure 8. COC of SVeC and PSS in a Test System

connected to the network. Full particulars of the test system are given in (Sauer & Pai, 1998). The outcome results were accomplished with the help of MATLAB. IEEE Type-I exciter is considered for all 3 generators. The performance of test system is checked by means of eigen-value analysis and non-linear time-domain simulation results under nominal load conditions are discussed in the following sections. The generator operating and loading conditions at nominal load are presented in Appendix.

In this section, the parameters of PSS and SVeC damping controllers can be chosen as identical capacities, uniform damping, i.e 0.01 is assumed for all machines, compensation level is 50%, and σ_0 is -0.5. The input signal

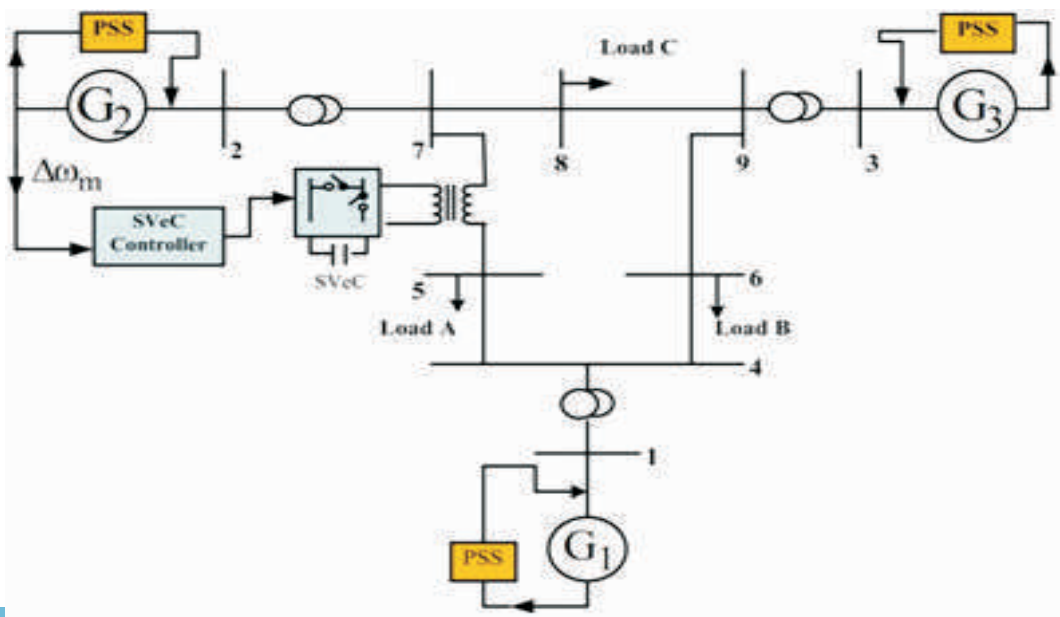

Figure 9. COC of Study System

www.manaraa.com

to the transmission line is selected as active power. The active power flow data are given in Table 1. The largest power flow in line 5-7 is considered as under study. So, the best location to place the SVeC is 5-7 installed in series with the line (Himaja et al., 2016).

3.1 Eigen-value Analysis

Table 2 lists the eigen-values of test system without control, total 21 eigen-values are present. In the total of 21 eigen-values, two has zero magnitude, three are real, and the remaining 16 are complex conjugate.

The eigen-values for W.S.C.C system without damping controller is most similar to with those described in (Sauer & Pai, 1998). In Table 2, without damping controller, the important dominant mode is (-0.1906 ± j 8.3666) and has the DR of 0.022 and therefore this mode has been referred to as critical swing mode. This DR can be improved by COC of SVeC and PSS to the network. So, the critical swing mode is shifted to a most desirable position in the s plane.

Table 3 lists the eigen-values of test system for COC of SVeC and PSS. The SVeC and PSS data are presented in Appendix. In the COC of SVeC and PSS results, 26 eigen-values are present. It has been observed that the critical swing mode ($\Lambda_{3,4}$) has been moved to (-0.3553 ± i 8.7223) on the imaginary axis of the complex s plane and has the DR of 0.0407. Additional improvement of damping in the COC of SVeC and PSS is 0.0187.

It is observed that the COC of SVeC and PSS can simultaneously improve the damping of the test system compared to the no control and influences the EPS stability.

3.2 Time-Response Analysis

The non-linear time-response result has been checked with COC of SVeC and PSS without the damping controller. The rotor angle and angular speed response has been plotted in Figure 10, where ω_1, ω_2, and ω_3 are the rotor speed of machines 1, 2, and 3, respectively. Similarly δ_1, δ_2 and δ_3, are the rotor angles of machine 1, 2, and 3, respectively. Figures 10 (a) to (d) indicate the capability of the proposed COC of SVeC and PSS control in reducing the settling time, peak overshoot, and damping LFO.

The performance of any network can be checked with settling time and peak overshoot. For better results, the peak overshoot should be minimized with settling time. From Table 4, it is observed that the COC of SVeC and PSS provides better results in terms of settling time, peak over shoot to damp rotor angle oscillations compared to without controller. Figures 10(a) and 10(b) show the responses of the angular velocity.

From Bus	To Bus	Real Power (p.u)
4	6	0.3070
6	9	0.6082
4	5	0.4094
5	7	0.8662
7	8	0.7638
8	9	0.2410

Table 1. Base Case (line flow) on 100 MVA Base

Mode	Without Control	Damping Ratio (ζ)	Frequency (rad/s)
$\Lambda_{1,2}$	-0.7195 ± j12.745	0.056	12.8
$\Lambda_{3,4}$	-0.1906 ± j 8.3666	0.022	8.37
$\Lambda_{5,6}$	-5.6804 ± j 7.9656	0.581	9.78
$\Lambda_{7,8}$	-5.3625 ± j7.9308	0.56	9.57
$\Lambda_{9,10}$	-5.2280 ± j 7.8259	0.555	9.41
$\Lambda_{11,12}$	-5.1777, -3.3983	1,1	5.18, 3.399
$\Lambda_{13,14}$	-0.4511 ± j 1.2003	0.352	1.28
$\Lambda_{15,16}$	-0.4478 ± j 0.7295	0.523	0.856
$\Lambda_{17,18}$	-0.4362 ± j 0.4871	0.667	0.654
$\Lambda_{19,20}$	0.0000,0.0000	1,1	0,0
Λ_{21}	-3.1250	1	3.125

Table 2. Eigen-values of Test System without Control

Mode	COC of SVeC and PSS		
	Eigenvalue	Damping Ratio	Frequency (rad/s)
$\Lambda_{1,2}$	-0.8443 ±12.847i	0.0656	12.9
$\Lambda_{3,4}$	-0.3553 ± 8.7223i	0.0407	8.73
$\Lambda_{5,6}$	-5.5534 ±7.8673i	0.577	9.63
$\Lambda_{7,8}$	-5.2584 ± 7.7544i	0.561	9.37
$\Lambda_{9,10}$	-5.2410 ± 7.8507i	0.555	9.44
Λ_{11}	-5.1544	1	5.1544
Λ_{12}	-3.4049	1	3.4049
$\Lambda_{13,14}$	-0.3935 ± 1.2149i	0.308	1.28
$\Lambda_{15,16}$	-0.4188 ± 0.7466i	0.489	0.856
$\Lambda_{17,18}$	-0.4064 ± 0.6092i	0.555	0.732
$\Lambda_{19,20}$	-0.1, -9.0909	1,1	0.1, 9.09
$\Lambda_{21,22}$	0, -9.1318	1,1	0, 9.1318
$\Lambda_{23,24}$	-9.0919, -9.1607	1,1	9.092, 9.161
$\Lambda_{25,26}$	-0.0766, -3.125	1,1	0.0766, 3.125

Table 3. Eigen-values of Test System for COC of SVeC and PSS

www.manaraa.com

From the results, the COC of SVeC and PSS is a more effective controller than without control to damp LFO.

Conclusion

In this study, SVeC acts as a novel series FACTS device to modify the line reactance and provides additional damping to critical modes. The mathematical analysis and current injection model of SVeC has been presented. A brief comparison of a new series FACTS device equipped with a POD stabilizer without controller is examined for damping LFO. The approach is verified by means of eigen-value analysis and time-response results. At nominal load, the eigen-values has been examined and the time-response results at without control and COC of SVeC and PSS are compared. The results obtained for a W.S.C.C test system demonstrates the applicability of the proposed controller and its ability to damp LFO at nominal loading condition.

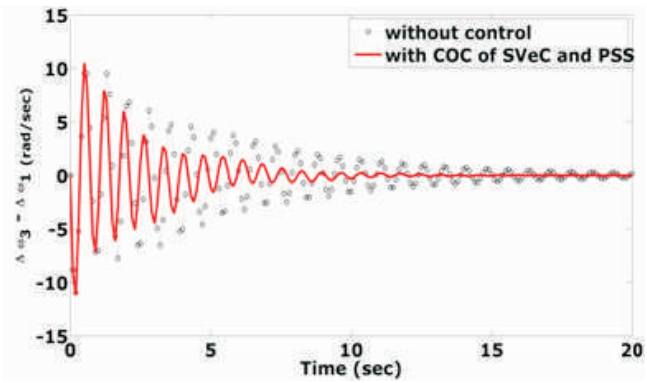

(a) Deviation in Angular Velocity $\Delta\omega_{31}$

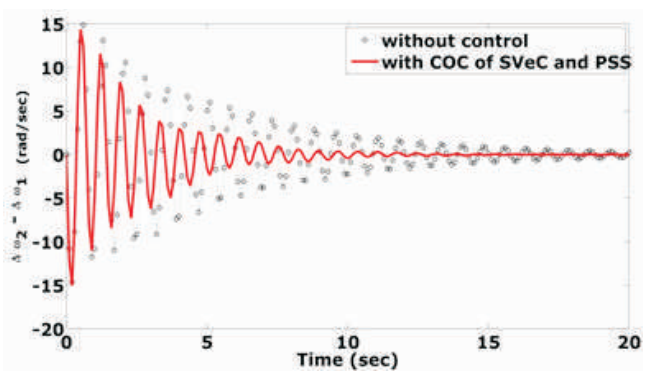

(b) Deviation in Angular Velocity $\Delta\omega_{21}$

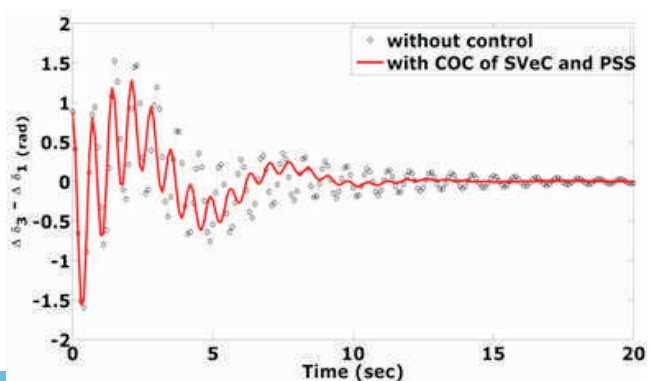

(c) Deviation in Generator Rotor Angle $\Delta\delta_{31}$

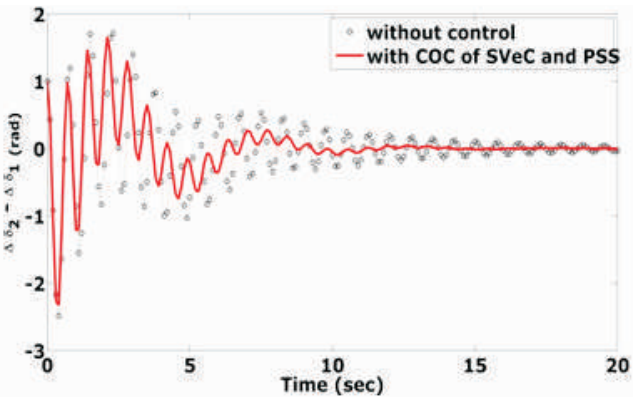

(d) Deviation in Generator Rotor Angle $\Delta\delta_{21}$

Figure 10. Rotor Angle and Angular Velocity Responses of the System without Controller and COC of SVeC and PSS

Name of the controller	% of peak overshoot			
	$\omega_3 - \omega_1$	$\omega_2 - \omega_1$	$\delta_3 - \delta_1$	$\delta_2 - \delta_1$
System without control	2.534 %	3.95 %	0.84 %	0.95 %
System with COC of SVeC and PSS	2.674%	3.67 %	0.66 %	0.88 %
	Settling time in Seconds			
System without control	19.75	19.78	18.82	18.81
System with COC of SVeC and PSS	11.00	11.01	11.21	10.55

Table 4. % of Peak Overshoot and Settling Time of Test System for without Control and with Coordinated Control of SVeC and PSS

References

[1]. Gonzalez, J. M., Canizares, C. A., & Ramirez, J. M. (2010). Stability modeling and comparative study of series vectorial compensators. *IEEE Transactions on Power Delivery*, 25(2), 1093-1103.

[2]. Himaja, K., Surendra, T. S., & Kalyani, S. T. (2016). Coordinated design of PSS and Series vectorial compensator controllers for damping power system oscillations. *Journal of Electrical Engineering*, 16(4), 507-512.

[3]. Kundur, P., Balu, N. J., & Lauby, M. G. (1994). *Power System Stability and Control* (Vol. 7). New York: McGraw-hill.

www.manaraa.com

[4]. **Lopes, L. A., & Joos, G. (2001).** Pulse width modulated capacitor for series compensation. *IEEE Transactions on Power Electronics*, 16(2), 167-174.

[5]. **Mancilla-David, F., Bhattacharya, S., & Venkataramanan, G. (2008).** A comparative evaluation of series power-flow controllers using DC-and AC-link converters. *IEEE Transactions on Power Delivery*, 23(2), 985-996.

[6]. **Padiyar, K. R. (1996).** *Power System Dynamics Stability and Control.* Singapore: Wiley.

[7]. **Pal, B., & Chaudhuri, B. (2006).** *Robust Control in Power Systems*. Springer Science & Business Media.

[8]. **Sadikovic, R. (2004).** *Damping controller design for Power System Oscillations, Internal Report*. 1-14.

[9]. **Safari, A., Shayeghi, H., & Shayanfar, H. A. (2016).** Coordinated control of pulse width modulation based AC link series compensator and power system stabilizers. *International Journal of Electrical Power & Energy Systems*, 83, 117-123.

[10]. **Sauer, P. W., & Pai, M. A. (1998).** *Power System Dynamics and Stability.* New Jersey : Prentice-Hall.

[11]. **Truong, D. N., & Wang, L. (2013, May).** Dynamic stability enhancement of a single-machine infinite-bus system using a series vectorial compensator. In *Industrial Electronics (ISIE), 2013 IEEE International Symposium on* (pp. 1-6). IEEE.

[12]. **Venkataramanan, G., & Johnson, B. K. (2002).** Pulse width modulated series compensator. *IEE Proceedings-Generation, Transmission and Distribution*, 149(1), 71-75.

[13]. **Wang, L., & Truong, D. N. (2012).** Application of a SVeC and a SSSC on damping improvement of a SG-based power system with a PMSG-based offshore wind farm. In *Power and Energy Society General Meeting, 2012 IEEE* (pp. 1-7). IEEE.

Appendix

Generator operating conditions (In p.u)			Generator loading conditions (In p.u)		
Generator	P	Q	Generator	P	Q
G_1	0.72	0.27	A	1.25	0.50
G_2	1.63	0.07	B	0.90	0.30
G_3	0.85	-0.11	C	1.00	0.35

Table 1A. Generator Operating and Loading Conditions at Nominal Load

X_L	X_C	T_1	T_2	$X_{s,max}$	$X_{s,min}$	K_{SVeC}
0.0269	0.5 p.u	0.15 s	0.11s	0.1	-0.1	20

Table 1B. SVeC Data

T_1	T_2	K_{PSS}
0.15 s	0.11s	20

Table 1C. PSS Data

www.manaraa.com

ABOUT THE AUTHORS

K. Himaja is currently working as a Lecturer in the Department of Technical Education at Government of Andhra Pradesh, India and also pursuing Ph.D. in the Department of Electrical Engineering at JNTU Hyderabad, India. She received the B.Sc. Degree in Electrical and Electronics Engineering from College of Engineering, Osmania University, Hyderabad and the M.Sc. Degree from JNTU, Hyderabad in 2008. Her area of interest, includes Power Electronics and Drives, FACTS, and Artificial Neural Networks.

Dr. T. S. Surendra is presently working as a Director at Visionary Lighting and Energy India (P) Ltd at Hyderabad and Chief Advisor of Solar Skill Development programs at the Surabhi Educational Society, Hyderabad, India. He received his B.Sc. Degree in Electronics Engineering from MCEME, Secundrabad, M.Sc. from Indian Institute of Technology (IIT) Delhi, India, and Ph.D Degree from JNTU Hyderabad, India. He has wide experience of about fifty years in the Army (Corps of Electronics and Mechanical Engineering), Industry and the Academia. He was nominated as a World Bank resource person for training in solar photovoltaic's systems in 1996.

Dr. S. Tara Kalyani is currently working as a Controller of Examinations and Professor in the Department of Electrical and Electronics Engineering at JNTU Hyderabad, India. She received her B.E Degree in Electrical and Electronics Engineering from Osmania University, Hyderabad and Ph.D. Degree from Jawaharlal Nehru Technological University (JNTU) Hyderabad, India. She has published a number of technical research papers in National & International Journals. Her research interests, include FACTS Controllers, Power Electronics Industrial Drives, and Energy Systems.

www.manaraa.com

Reproduced with permission of copyright owner. Further reproduction prohibited without permission.

www.manaraa.com